DOI: 10.1002/adem.((please add manuscript number))

Lithography and etching-free microfabrication of silicon carbide on insulator using direct UV laser ablation*

Tuan-Khoa Nguyen[1‡], Hoang-Phuong Phan[1‡], Karen M. Dowling[2], Ananth Saran Yalamarthy[2], Toan Dinh[1,3], Vivekananthan Balakrishnan[1], Tanya Liu[4], Caitlin A. Chapin[5], Quoc-Dung Truong[6], Van Thanh Dau[7], Kenneth E. Goodson[4], Debbie G. Senesky[2,5], Dzung Viet Dao[7], and Nam-Trung Nguyen[1]*

((Optional Dedication))

[1] *Queensland Micro and Nanotechnology Centre, Griffith University, Queensland, Australia*
[2] *Department of Electrical Engineering, Stanford University, California, USA*
[3] *School of Mechanical and Electrical Engineering, University of Southern Queensland, Queensland, Australia*
[4] *Department of Mechanical Engineering, Stanford University, California, USA*
[5] *Department of Aeronautics & Astronautics, Stanford University, California, USA*
[6] *BOSCH Automotive R&D Center, Deutsches Haus, Ho Chi Minh city, Vietnam*
[7] *School of Engineering and Built Environment, Griffith University, Queensland, Australia*

[*] *E-mail:* k.nguyentuan@griffith.edu.au, h.phan@griffith.edu.au
[‡] *T.-K. Nguyen and H.-P. Phan contributed equally to this work.*

This work was performed in part at the Queensland node of the Australian National Fabrication Facility (ANFF), a company established under the National Collaborative Research Infrastructure Strategy to provide nano and microfabrication facilities for Australia's researchers. NTN and DVD acknowledge funding support from the Australian Research Council grants LP160101553, LP150100153, and LE190100066.

Abstract

SiC (silicon carbide) -based micro systems are promising alternatives for silicon-based counterparts in a wide range of applications aiming at conditions of high temperature, high corrosion, and extreme vibration/shock. However, its high resistance to chemical substances makes the fabrication of SiC particularly challenging and less cost effective. To date, most SiC micromachining processes require time-consuming and high-cost SiC dry-etching steps followed by metal wet etching, which slows down the prototyping and characterization process of SiC devices. This work presents a lithography and etching-free micro fabrication for SiC on insulator based MEMS devices. In particular, we employ a direct laser ablation technique to replace the conventional lithography and etching processes to form functioning SiC devices from SiC-on-glass wafers. Utilizing a single line-cutting mode, both metal-contact shapes and

SiC micro structures can be patterned simultaneously with a remarkably fast speed of over 20 cm/s. As a proof of concept, we demonstrated several SiC micro devices including temperature sensors, strain sensors, and micro heaters, showing the potential of the proposed technique for rapid and reliable prototyping of SiC-based MEMS.

Keywords: force sensor, laser ablation, micro heater, temperature sensor, silicon carbide

1. Introduction

Silicon carbide (SiC) has been attracting a significant interest from the microelectromechanical systems (MEMS) community owing to its superior physical properties and resilience over Si in harsh environmental applications.[1-3] The advantages result from the high energy band gap, mechanical strength, chemical inertness, and the high melting point of SiC [4-6]. Therefore, a wide range of silicon carbide based micro sensing/electronics devices have been developed with several micro-machining techniques.[7-8] Unlike silicon counterparts, silicon carbide micro-machining processes are undoubtedly limited and expensive due to the chemical inertness of SiC. For instance, SiC wet etching processes typically requires extreme conditions and aggressive chemicals.[9] Moreover, in terms of patterning bulk SiC wafers, dry etching of SiC using plasma based processes results in a very low etching rate, hindering the implementation of SiC micro/nano electronic and sensing devices on a large scale. To mitigate this obstacle, epitaxially grown silicon carbide on silicon substrates has been introduced and proven to be a promising approach, since it only requires patterning of thin SiC layers that is more favorable than that of bulk SiC wafers. Compared to other polytypes such as 4H-SiC and 6H-SiC, the cubic SiC is the most suitable polytype for micro sensing applications. This is owing to its capability of deposition on a Si substrate, making it compatible with MEMS process as well as reducing the cost of the material compared to the bulk counterparts. Additionally, this platform can benefit from the mature Si-based fabrication processes such as etching of the Si substrate, making it convenient for engineering SiC-based micro systems. Thanks to technological developments in the growth process of SiC on Si, high quality and large scale epitaxial SiC on Si wafers have been introduced.[10] However, the leakage of the electric current through the SiC-Si junction drastically increases with temperature, exposing a significant limitation for high temperature applications that SiC materials are used for. To overcome this obstacle, SiC thin film can be bonded onto insulating substrates such as glass by wafer bonding to prevent current leakage at high temperature.[11-14] This platform provides a feasible development for SiC electronics, eliminating the leakage occurred in SiC-on-Si electronics at high-temperature operations. Previously, we introduced an anodic bonding

technique for as-grown SiC-on-Si onto an insulating substrate (i.e. glass), indicating a great potential for SiC bases sensors and electronics for a wide range of application including biological utilizations.[11]

To achieve SiC micro/nano structures, expensive micro/nano machining processes in tightly controlled cleanroom environments are typically required,[15-16] which includes lithography processes followed by plasma/wet etching of SiC micro/nano structures. These strict requirements are significant obstacles for the developments of cost effective SiC-based sensors and electronics devices, hindering the fundamental characterization of the SiC materials. The present work reports a novel method for rapid prototyping of SiC micro-scale sensors and electronics using UV laser ablation, to extend the application potential of the SiC-on-glass platform. We demonstrate that the proposed technique can be used to fabricate multifunctional SiC micro devices including temperature/force sensors as well as integrated heaters, which can work at elevated temperatures. The simplified method eliminates sophisticated lithography and etching processes with cleanroom facilities, showing the potential in reducing the fabrication cost of SiC-based micro-scale sensors and electronics. This approach paves the way for fast-prototyping, cost effective SiC-based micro sensing and heating devices for harsh environmental applications.

2. Lithography and etching free fabrication of SiC-on-glass

Figure 1 shows the concept of the fabrication process using laser ablation starting from a SiC-on-glass wafer. Silicon carbide films were initially epitaxially grown on a (100) Si wafer by low pressure chemical vapor deposition (LPCVD) process and doped with nitrogen to achieve n-type SiC. In our previous work, we have reported that the as-grown SiC film on a Si wafer is single crystalline 3C-SiC and its crystallographic orientation is (100) by selected area diffraction (SAD) and X-ray powder diffraction (XRD) measurements, respectively.[17] Due to the mismatch in lattice constant and thermal expansion of SiC and Si, we observed the stacking fault defects at the SiC/Si interface. However, the stacking faults mainly distributed within 50 nm from the SiC/Si interface and the crystallinity significantly improved with increasing the SiC film thickness. The carrier concentration of the SiC thin film was measured to be 10^{18} cm^{-3} by a hot-probe technique. The resistivity of the SiC film was 8 Ω.μm. Subsequently, the as-grown 600-nm SiC thin films were transferred onto an insulating substrate by anodic bonding. The details of the transferring process of SiC onto an insulating substrate can be found elsewhere.[11]

Next, a 200-nm nickel (Ni) layer was selectively deposited on top of the 600-nm SiC layer using a shadow mask, forming a Ni layer only in desired electrode areas, Fig. 1(c). Micro patterns of SiC were then formed by laser scribing with a diode-pumped solid state (DPSS) Samurai^{TM} laser (355 nm wavelength) at an average power of 2 Watt. The Ni layer was also cut to confine the metal-electrode pads. The cutting mode for both SiC and Ni was chosen as single-cut lines at 50% of the full power setting (~3 Watt) with a scanning speed of 200 mm/s, forming trenches on the glass substrate, which electrically isolates SiC devices from each other. The SiC micro-structure designs, created using a standard computer-aided design (CAD) software, were aligned with the pre-deposited electrode areas using the printing-preview mode and a home-built camera system. Since the laser only etches the boundary (i.e. perimeter) of each SiC micro structure, the total fabrication time is extremely short. For instance, the fabrication of an array of ten SiC U-shape resistors with a total perimeter of 120 mm took less than 5 s. In addition, movable structures of SiC such as one-side clamped cantilevers or double-sided clamped bridges can also be formed because the UV laser can also remove the glass substrate, enabling rapid prototyping of SiC-based mechanical sensors and electronics. In cleanroom-based fabrication processes, SiC sensors and electrodes are patterned through the deposition/development of photoresist followed by SiC and/or metal etching. In contrast, our direct laser ablation of SiC only requires a single cutting step, which significantly reduces the fabrication time and eliminates material and chemical costs associated with the lithography and etching processes arising from conventional micro-machining fabrications. With this new method, the post-etching process (e.g. photoresist removal) is no longer required, allowing for the fabrication of SiC-on-glass micro electronics devices in typical laboratory conditions without the need for cleanroom facility. The fabricated SiC structures can be utilized as a multi-functional sensing and heating platform for numerous applications.

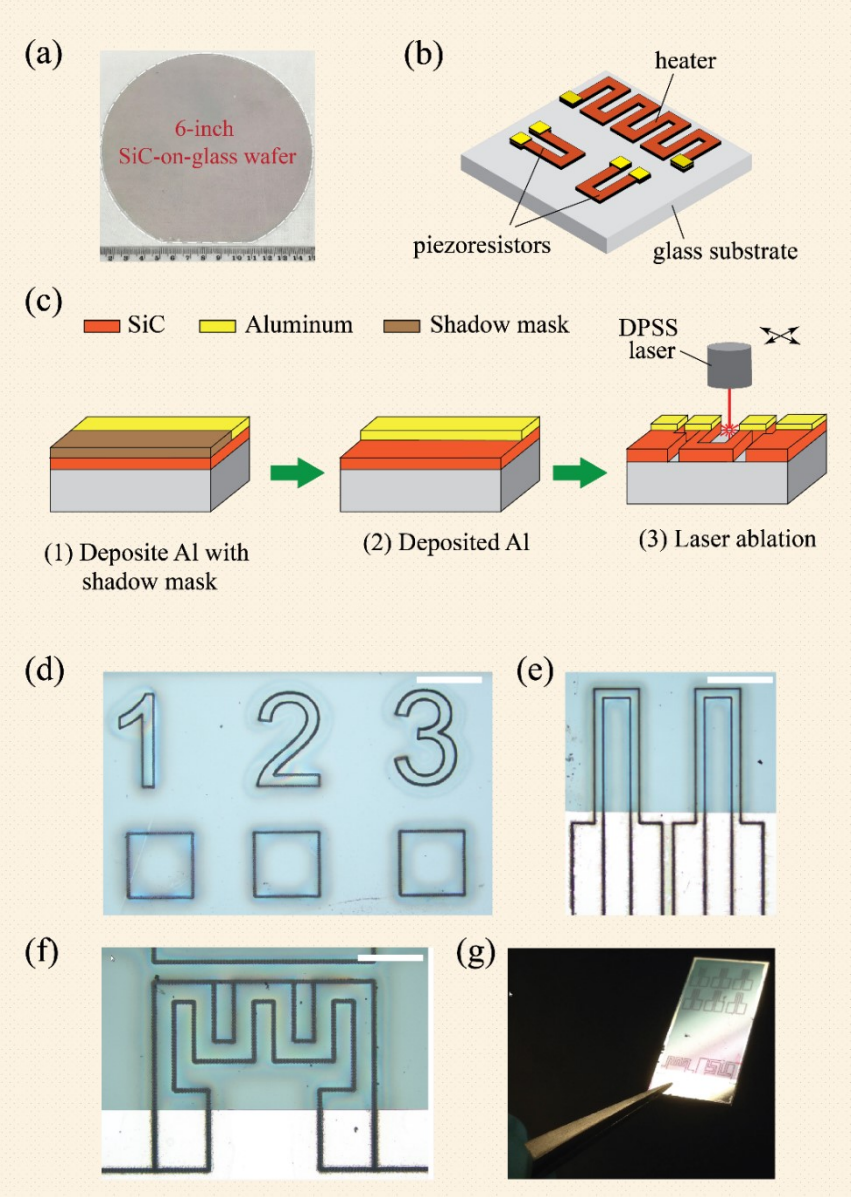

Figure 1: Concept of the lithography-free process to form SiC micro devices. (a) Photograph of 6-inch SiC-on-glass wafer (SiC film was transfered onto glass from a (100) SiC-on Si wafer). (b) Schematic sketch of direct laser ablation fabrication technique. (c) Fabrication steps using a shadow mask to form patterned metal contacts, followed by computer-aided control laser ablation to create various patterns of piezoresistors and micro heaters. (d) Patterned structures from SiC-on-glass wafer. (e) U-shape resistors for temperatrure and force sensors. (f) Spring-shaped micro heater; the metal contact areas are shown as white color; scale bar for (d), (e), (f): 500 µm. (g) Photograph of multifuntional chip consisting of various type of micro-scale sensors and heaters using the laser ablation method.

3. Demonstration of laser-engraved SiC applications

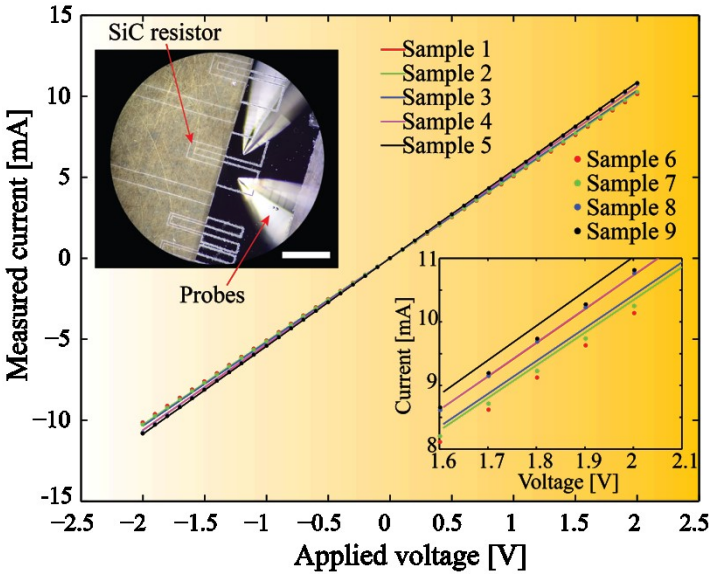

Figure 2: Current-voltage (I-V) characteristics of the fabricated SiC resistors at room temperature (~18°C). The test was conducted with 9 samples in which the I-V characteristic are almost identical for all tested SiC resistors. The data indicate the uniformity and consistency of the laser ablation in patterning SiC structures. Inset: Top-left: Microscopic photograph of U-shaped SiC structures on the transparent glass substrate (dark-color regions are metal contacts), scale bar, 1,000 μm. Bottom-right: Zoom-in view of the I-V curve at voltage from 1.6-2.1 V.

Since UV laser can penetrate and remove the SiC thin film and glass layers, it is convenient and cost effective to form SiC-based sensors/heaters in one single-step fabrication. Figures 1(d),(e),(f) show images of the fabricated SiC structures including text patterns, U-shaped resistors, a spring-shaped heater on a SiC-on-glass chip (Fig. 1(g)). The current-voltage characteristic of the as-fabricated SiC resistors was measured using a digital multimeter (i.e. Agilent™ B1500), indicating an excellent Ohmic contact between metal and SiC, Fig. 2. The resistance of SiC was measured with 9 samples, showing a small deviation of less than 5%. This result indicates the uniformity of SiC devices fabricated using a single-step UV laser ablation. Furthermore, since SiC was transferred onto a glass substrate, the problem of current leakage into the substrate was completely solved, enabling the development of SiC-based high temperature sensing devices. The following sub sections demonstrate several MEMS applications of our laser ablation technique including temperature sensors, micro heaters, and force sensors.

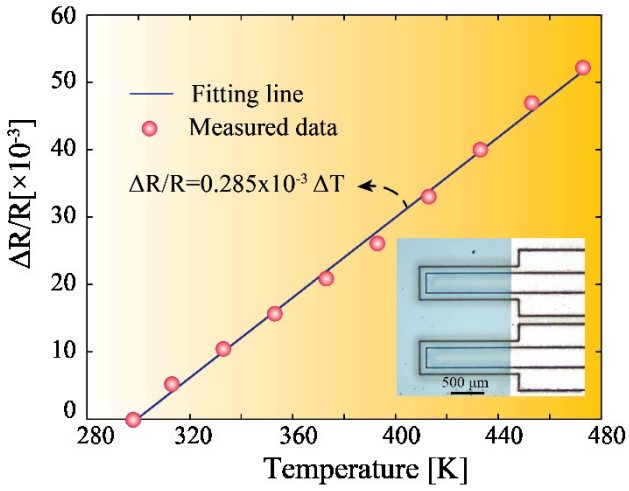

Figure 3: Characterization of SiC-on-glass temperature sensors: The resistance variation is in a linear regression with the increasing temperature from 293 K to 473 K indicating the merit of the as-fabricated SiC structures for temperature sensing. Inset: Microscopic photograph of SiC temperature sensors.

3.1. Temperature sensors

Owing to its resilience to high temperature and the significant thermoresistive effect, the SiC-on-glass platform can be utilized as a sensitive temperature sensor. The measurement of the SiC-on-glass temperature sensors was conducted in an oven with precisely controlled temperature of ± 0.1 °C. The resistance change of the SiC sensor was measured against temperature in the range from room temperature to 473 K. The temperature was increased by 20 °C per step and the resistance of SiC was recorded using a digital multimeter (i.e. Agilent™ B1500). Figure 3 shows that the resistance of the SiC sensor significantly increases with the increasing temperature at the testing range. It should be pointed out that the increment in the resistance of the SiC indicates that the decrease in electron mobility plays is more dominant than the increase in thermally activated carrier concentration that reduces the resistance. The reduction of the electron mobility at elevated temperatures is due to electron-electron, and electron-phonon scattering, which is more dominant in highly doped semiconductors. The thermal resistive effect in SiC films can be quantified by the temperature coefficient of resistance, $TCR = \frac{\Delta R}{R\Delta T}$. Accordingly, the TCR in the highly doped SiC-on-glass was found to be 285 ppm/K.

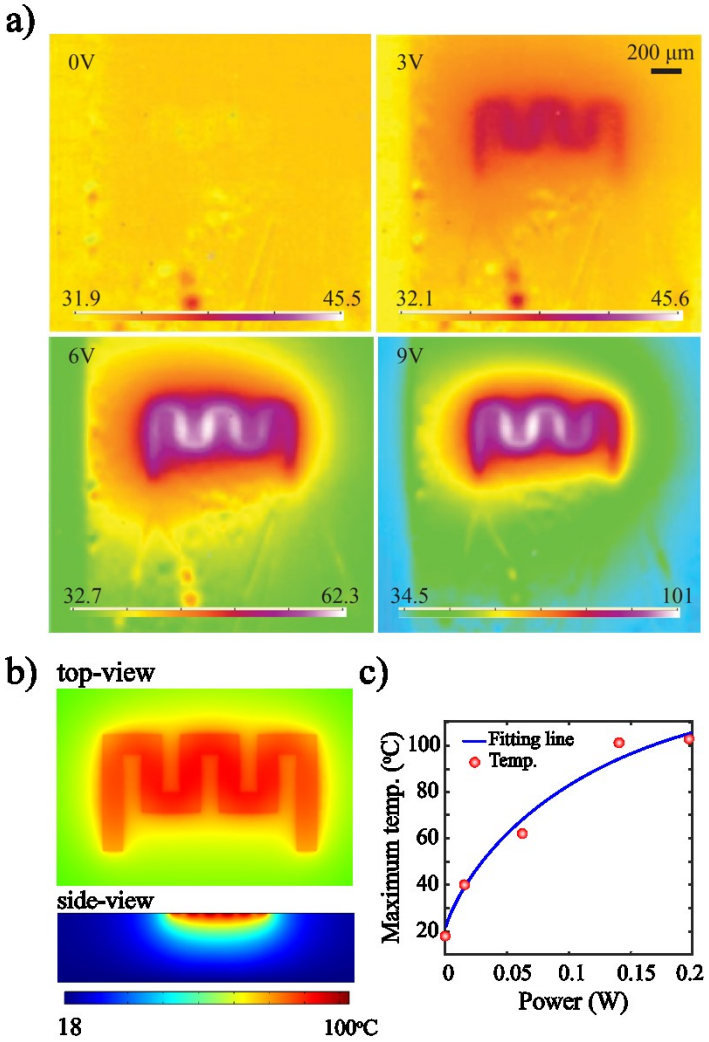

Figure 4: Demonstration of spring-shaped SiC micro heater employing Joule heating effet (Unit of the scale bar: °C): a) Thermal image of the sensor under an applied voltage of 0, 3, 6, 9V using an infrared camera (QFI InfraScope™ II) at an ambient temperature of 18 °C. b) Finite element analysis of SiC heater on glass substratre at an applied voltage of 9V. c) Relationship between maximum generated temperature of the heater versus supplied power.

3.2. Micro heaters

Micro heaters can be employed as the heat source of mass-flow sensors or to provide thermal stimuli to bio-species grown on SiC, thanks to the good bio-compatibility of SiC.[18-21] Since the glass substrate is an excellent electrical insulator, the use of SiC-on-glass heaters will confine heating power on the SiC resistors, locally raising temperatures at the targeted areas due to the Joule heating effect. We applied a voltage to a spring-shape SiC and observed its temperature change using an infrared (IR) microscope to demonstrate the function of SiC-on-

glass heaters. Prior to applying the voltage to the SiC resistors, the surface of SiC was coated with a carbon powder layer with a known emissivity which was calibrated by varying the surface temperature of this coating layer using a hot plate. This calibrated emissivity (ranging from 0.92 to 0.98) was employed to derive the actual temperature generated from the SiC heaters under applied DC voltages. Figure 4 presents the temperature of the SiC heater at 0, 3V, 6V, and 9V, for which the temperature of the heater can reach above 100 °C under an applied power of 0.15 W. The measured temperature distribution is in good agreement with a finite element analysis (FEA) with a conductivity of SiC of 1.25×10^5 S/m, Fig. 4(b). In the FEA model, the SiC layer with a thickness of 600 nm on top of 1-mm thick glass substrate. The basic mechanical, electrical and thermal properties of the glass layer was derived from integrated parameters within the software (i.e. COMSOL™ Multiphysics) (also available elsewhere). The Young' modulus and thermal conductivity SiC are set as 350 GPa, and 350 W/(m.K), respectively; the electrical conductivity of SiC is calculated from its resistivity: $\sigma=1/\rho=1.25\text{x}10^5$ S/m. The measured temperature of the glass substrate at the vicinity of the SiC heater was slightly higher than the simulation result, which is attributed to an increase in the thermal conductance caused by the carbon coating layer.

Figure 4(c) shows the relationship between the maximum temperature generated using the spring-shaped SiC micro heater versus the applied electric power. The heater can generate a high temperature with a relatively small supplied power. This is due to the nearly zero leakage current from SiC to the glass substrate, in which the electrical current only flows in the SiC heater. Therefore, the integrated SiC heater at a relatively low voltage/power shows a promising feature for bio cell thermal stimulation applications (e.g. cell lysis), which also takes advantage of the robustness of SiC with chemical or biological environment.[22]

3.3. Micro force sensors

To characterize the SiC-based force sensors, mesa SiC resistors on a SiC-on-glass beam were formed in an U-shape with a longitudinal edge (parallel to the beam's length) much larger than the transverse one (perpendicular to the beam's length), Fig. 3. The fabricated SiC structures can be employed as a force sensitive sensor owing to the large piezoresistance of SiC.[23-24] The bending beam method was employed to measure a targeted force if it is applied to a free end of the beam and induces uniaxial strain onto SiC resistors located on beam-shaped SiC-on-glass chips (length, width and thickness are 15 mm × 2 mm × 0.5 mm). The SiC piezoresistors are located at the vicinity of the other end of the cantilever, which is clamped, in order to yield the highest possible induced strain.

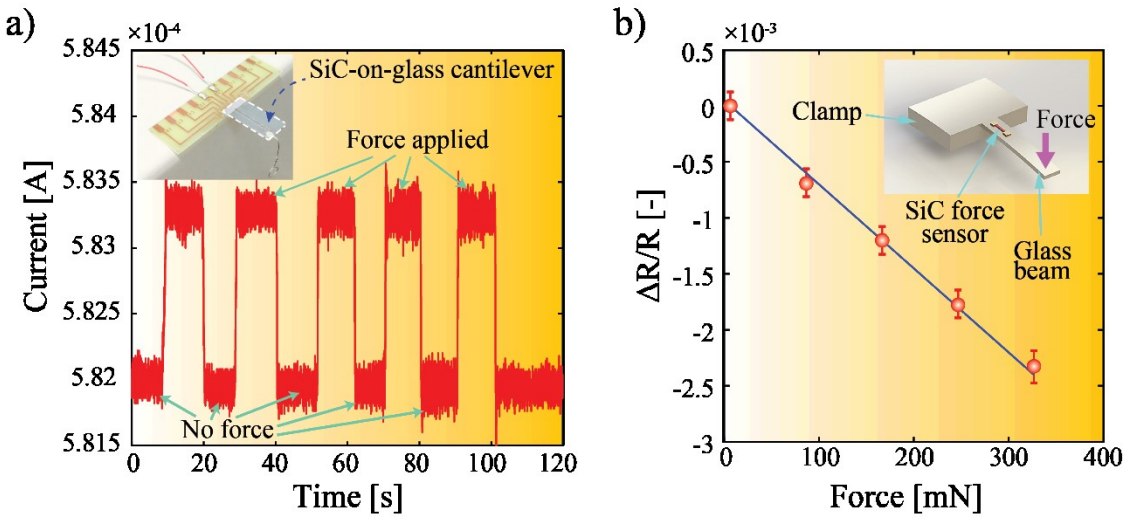

Figure 5. Demonstration of SiC force sensors. (a) the change of electric current under a constant applied force (F=320 mN). Inset: Bending beam method was employed to measure applied forces. (b) Resistance change of SiC force sensor under incremental forces (80 mN per step). Inset: Sketch of SiC force sensor test.

Figure 5(a) shows the variation of the output electrical current with respect to an applied force of 320 mN (at a supplied voltage of 0.1 V). At the force application state, the electrical current flowing through the SiC sensor significantly increased and remain stable in the duration of the applied force. This indicates that the resistance of the SiC sensor decreases with the applied strain, showing a negative gauge factor ($GF = \frac{\Delta R/R}{\varepsilon}$). As the applied strain can be derived by,[25] $\varepsilon = \frac{6FL}{Ewt^2}$, where F is the applied force, L, b and t are the length, width and thickness of the SiC-on-glass beam, E is the Young modulus of glass, E = 75 GPa. Consequently, the GF of the n-type SiC was found at -10.3, which is equipvalent to the GFs of other SiC strain sensors fabricated using conventional lithography processes.[14, 26] If the force was completely removed, the electrical current instantaneously returned back to its original value without any drift or hysteresis under tens of applying cycles. This characteristic shows the good repeatability and fast response of the SiC force sensor.

To confirm the linearity of the SiC force sensor, a stepped loading from 0 to 320 mN with an interval of 80 mN was then applied. Figure 5(b) clearly shows that the linear change in the current with the applied force exhibited the excellent linearity of the sensor in measuring force and strain. The good linearity and repeatability of the SiC force sensor demonstrate the

potential of our simple fabrication technique in the development of SiC-based mechanical sensors.

4. Conclusion

We demonstrate a single-step and cost-effective fabrication technique to form SiC micro structures on an insulating substrate for a MEMS-based multifunctional platform consisting of micro-scale sensors and heaters utilizing direct laser ablation. This method eliminates the requirement for sophisticated lithography and etching processes in a cleanroom facility, reducing the cost associated with micro-machining fabrications as well as allow fast prototyping SiC-based structures for MEMS applications. As a proof of concept, we designed and tested multifunctional SiC-based micro heaters, temperature and force sensors on a single chip. The developed micro sensors exhibited high sensitivity and good repeatability/linearity while the integrated heater can effectively generate a temperature of up to 100 °C with a relatively low power. This SiC-based multifunctional platform is promising for a wide range of sensing and heating applications at the micro scale utilizing the fast prototyping capability of direct UV laser ablation.

References

[1] C.-M. Zetterling, *MRS Bull.* **2015**, 40, 431.
[2] X. Lu, J. Y. Lee, Q. Lin, *Sci. Rep.* **2015**, 5, 17005.
[3] H.-P. Phan, T.-K. Nguyen, T. Dinh, A. Iacopi, L. Hold, M. J. A. Shiddiky, D. V. Dao, N.-T. Nguyen, *Adv. Eng. Mater* **2018**, 20, 1700858.
[4] X. L. Feng, M. H. Matheny, C. A. Zorman, M. Mehregany, M. L. Roukes, *Nano Lett.* **2010**, 10, 2891.
[5] H.-P. Phan, K. M. Dowling, T. K. Nguyen, T. Dinh, D. G. Senesky, T. Namazu, D. V. Dao, N.-T. Nguyen, *Mater. Des.* **2018**, 156, 16.
[6] D. G. Senesky, B. Jamshidi, C. Kan Bun, A. P. Pisano, *IEEE Sens. J.* **2009**, 9, 1472.
[7] T. Lehmann, J. Baier, A. Leineweber, A. Kienzle, J. Bill, *Adv. Eng. Mater* **2015**, 17, 1631.
[8] M. A. Lantz, B. Gotsmann, P. Jaroenapibal, T. D. B. Jacobs, S. D. O'Connor, K. Sridharan, R. W. Carpick, *Adv. Funct. Mater.* **2012**, 22, 1639.
[9] T.-K. Nguyen, H.-P. Phan, T. Dinh, K. M. Dowling, A. R. M. Foisal, D. G. Senesky, N.-T. Nguyen, D. V. Dao, *Mater. Des.* **2018**, 156, 441.
[10] L. Wang, S. Dimitrijev, J. Han, P. Tanner, A. Iacopi, L. Hold, *J. Cryst. Growth* **2011**, 329, 67.
[11] H. P. Phan, H. H. Cheng, T. Dinh, B. Wood, T. K. Nguyen, F. Mu, H. Kamble, R. Vadivelu, G. Walker, L. Hold, A. Iacopi, B. Haylock, D. V. Dao, M. Lobino, T. Suga, N. T. Nguyen, *ACS Appl. Mater. Interfaces.* **2017**, 9, 27365.
[12] C. Tudryn, S. Schweizer, R. Hopkins, L. Hobbs, A. J. Garratt-Reed, *J. Electrochem. Soc.* **2005**, 152, E131.
[13] J.-H. Lee, I. Bargatin, J. Park, K. M. Milaninia, L. S. Theogarajan, R. Sinclair, R. T. Howe, *J. Vac. Sci. Technol. B* **2012**, 30.

[14] H.-P. Phan, T.-K. Nguyen, T. Dinh, H.-H. Cheng, F. Mu, A. Iacopi, L. Hold, D. V. Dao, T. Suga, D. G. Senesky, N.-T. Nguyen, *Phys. Status Solidi A* **2018**, 215, 1800288.
[15] C. A. Zorman, R. J. Parro, *Phys. Status Solidi B* **2008**, 245, 1404.
[16] T. Dinh, T. K. Nguyen, H. P. Phan, Q. Nguyen, J. Han, S. Dimitrijev, N. T. Nguyen, D. V. Dao, *Adv. Eng. Mater* **2019**, 21, 1801049.
[17] A. R. Md Foisal, A. Qamar, H. P. Phan, T. Dinh, K. N. Tuan, P. Tanner, E. W. Streed, D. V. Dao, *ACS Appl. Mater. Interfaces.* **2017**, 9, 39921.
[18] V. Naglieri, B. Gludovatz, A. P. Tomsia, R. O. Ritchie, *Acta Mater.* **2015**, 98, 141.
[19] S. J. Schoell, M. Sachsenhauser, A. Oliveros, J. Howgate, M. Stutzmann, M. S. Brandt, C. L. Frewin, S. E. Saddow, I. D. Sharp, *ACS Appl. Mater. Interfaces.* **2013**, 5, 1393.
[20] J. Fan, H. Li, J. Jiang, L. K. So, Y. W. Lam, P. K. Chu, *Small* **2008**, 4, 1058.
[21] V. Balakrishnan, T. Dinh, T. Nguyen, H. P. Phan, T. K. Nguyen, D. V. Dao, N. T. Nguyen, *Rev Sci Instrum* **2019**, 90, 015007.
[22] H.-P. Phan, M. K. Masud, R. K. Vadivelu, T. Dinh, T.-K. Nguyen, K. Ngo, D. V. Dao, M. J. A. Shiddiky, M. S. A. Hossain, Y. Yamauchi, N.-T. Nguyen, *Chem. Commun.* **2019**, 55, 7978.
[23] J. Bi, G. Wei, L. Wang, F. Gao, J. Zheng, B. Tang, W. Yang, *J. Mater. Chem. C* **2013**, 1, 4514.
[24] X. Li, S. Chen, P. Ying, F. Gao, Q. Liu, M. Shang, W. Yang, *J. Mater. Chem. C* **2016**, 4, 6466.
[25] H.-P. Phan, T. Dinh, T. Kozeki, T.-K. Nguyen, A. Qamar, T. Namazu, N.-T. Nguyen, D. V. Dao, *IEEE Electron Device Lett.* **2016**, 37, 1029.
[26] T. Akiyama, D. Briand, N. F. de Rooij, *J. Micromech. Microeng* **2012**, 22, 085034.